Journal of Applied Electrochemistry (2006) 36:1091–1097
DOI 10.1007/s10800-006-9190-3

Electrochemical studies on nanofiller incorporated poly(vinylidene fluoride–hexafluoropropylene) (PVdF–HFP) composite electrolytes for lithium batteries

A. MANUEL STEPHAN[1,2], KEE SUK NAHM[1,*], M. ANBU KULANDAINATHAN[2], G. RAVI[3] and J. WILSON[3]
[1]*School of Chemical Engineering and Technology, Chonbuk National University, Chonbuk, 561-756, South Korea*
[2]*Central Electrochemical Research Institute, Karaikudi, 630 006, India*
[3]*Department of Physics, Alagappa University, Karaikudi, 630 003, India*
*(*author for correspondence, e-mail: nahmks@chonbuk.ac.kr)*

Received 17 February 2006; accepted in revised form 9 June 2006

Key words: compatibility: Lewis-acid base theory, composite polymer electrolyte, ionic conductivity

Abstract

Composite polymer electrolytes (CPE), comprising poly(vinylidene fluoride–hexafluoropropylene) (PVdF–HFP), aluminum oxyhydroxide, $(AlO[OH]_n$ – of 40 nm and 7 μm) as filler and $LiN(C_2F_5SO_2)_2$ or $LiClO_4$ as lithium salt were prepared using a solution casting technique. The membranes were subjected to XRD, impedance spectroscopy, compatibility and transport number studies. The incorporation of nanofiller greatly enhanced the ionic conductivity and the compatibility of the composite polymer electrolyte. The electrochemical properties of CPE with nano sized fillers are better than those of micron size. Charge- discharge studies of Li $Cr_{0.01}Mn_{1.99}O_4$/CPE/Li cells were made at 70 °C and are discussed.

1. Introduction

The rapid growth of the miniature electronic and computer-related industries has caused great demand for smaller and lighter batteries with improved safety, energy and power characteristics [1–3]. Lithium polymer batteries are expected to meet the above requirements and are thus considered as next-generation rechargeable batteries by virtue of their advantages such as improved safety, lower material costs, ease of fabrication into flexible geometries, and the absence of electrolyte leakage [4, 5]. Gel-type polymer electrolytes on the other hand, suffer from syneresis, a phenomenon by which the liquid component separates out from the host matrix in due course or upon application of pressure, which leads to leakage of electrolyte from the battery and related safety problems. Moreover polymer electrolytes loose their mechanical strength when plasticized [6–9]. The polymer films have to be hardened either by chemical or physical curing which results in high processing costs. In order to circumvent this problem Tarascon et al. [10] introduced a novel porous membrane in which the electrolyte can be embedded in the porous structure. One of the authors has made a series of studies on poly (vinlylidene fluoride) (PVdF–HFP) membranes by the phase inversion technique [11–16]. However, these membranes suffer from poor rate capabilities [17]. Recent studies reveal that composite polymer electrolytes alone can offer reliable and safe batteries [18–20]. Also of importance the Lewis-acid base interaction plays a vital role in enhancing the ionic conductivity of composite polymer electrolytes [21, 22]. Most studies have been made on poly(ethylene oxide) based electrolytes. Only a very few studies have been made on other polymer hosts such as poly (acrylonitrile) (PAN) [23], poly (methyl methacrylate)/poly(ethylene glycol diacrylate) [24] and fully amorphous trifunctional poly ether (3PEG) and poly (ethylene methylene oxide) (PMEG) electrolytes [25]. However, the transport number of composite polymer electrolytes was found to be very low (> 0.4). In the present study PVdF–HFP was used as a host because of its appealing properties. This polymer host itself has a high dielectric constant of 8.4 which assists higher dissociation of species. The PVdF crystalline phase acts as a mechanical support and the HFP amorphous phase facilitates higher ionic conduction. Also the inert filler, $AlO[OH]_n$, has a strong OH base for better interaction with the acidic species of the salt and polymer host.

It is reported [26] that composite electrolytes with nanosized fillers are more compatible and the electrochemical properties are much better than those of fillers of micron size. In order to study the influence of particle size on the ionic conductivity and electrochemical properties of the composite polymer electrolytes inert filler of two different sizes were used. Furthermore the

role of the anion on the ionic conductivity and other electrochemical properties in the polymer host has also been examined. Recent studies reveal [18–20] that lithium batteries with composite polymer electrolyte alone can offer safe and reliable batteries for elevated temperature applications especially for electric vehicle applications. Moreover the passivation of lithium is unpredictably influenced by the presence of liquid components/plasticizers in the gel. The liquid/plasticizer phase decomposes at the lithium surface, thereby eventually affecting the cycling performance. On the other hand, composite polymer electrolytes have no any liquid components in the matrix. Hence in the present study, $LiCr_{0.01}Mn_{1.99}O_4$/CPE/Li cells were assembled and their cycling profiles were examined at 70 °C and are discussed.

2. Experimental procedure

Poly (vinlylidene fluoride–hexafluoro propylene)(PVdF–HFP) (Kynar, Japan) and lithium bis perfluorosulfonyl imide, $LiN(C_2F_5SO_2)_2$ and $LiClO_4$ were dried under vacuum at 90 °C for 12 h before use. The inert filler, aluminum oxyhydroxide, $AlO[OH]_n$ of two different sizes (40 nm, 7 microns) (COBOT, USA) was dried at 120 °C for 12 h before use. The preparation of nano composite electrolyte involved the dispersion of the selected inert filler and $LiN(C_2F_5SO_2)_2/LiClO_4$ salt in anhydrous tetrahydrofuran (THF), followed by the addition of PVdF–HFP of different concentrations as shown in Table 1. The resultant solution was cast as film in an argon atmosphere. The solvent was allowed to evaporate and the composite film was obtained. The average film thickness was between 30 and 50 μm. This procedure yielded homogenous and mechanically strong membranes which were dried under vacuum at 80 °C for 24 h.

The films were sandwiched between two stainless steel discs of diameter 1 cm and the ionic conductivity of the membranes was measured using an electrochemical impedance analyzer (IM6 – Bio Analytical Systems, USA) in the 50–100 kHz frequency range at various temperatures viz., 0, 15, 30, 40, 50, 60,70 and 80 °C. The values of lithium transference number (t_{Li}^+) were measured by imposing a dc polarization pulse to a cell of the lithium-composite polymer electrolyte – lithium type and by following the time evolution of the resulting current flow using the expression [27]

$$t_{Li}^+ = I_s(V - I_0R_0)/I_0(V - I_sR_s) \quad (1)$$

where I_0 and I_s are the initial and steady–state currents, R_0 and R_s the initial and steady–state resistance of the passivated layers and "V" is the applied potential. AC impedance spectra were recorded before and after the current relaxation measurements without interruption of the Dc bias, to permit R_0 and R_s to be evaluated. In the present study the dc voltage pulse applied to the cell was 10 mV. The measurements were taken at the initial time of the applied dc voltage pulse ($t = t_o$, $R = R_o$, $l = l_o$) and under steady conditions ($t = t_s$, $R = R_s$, $l = l_s$) at 30 °C.

The compatibility of the Li/CPE/Li symmetric cells was investigated by studying the time dependence of the impedance of the systems at a open circuit at 70 °C [26]. In the present study sample S5 was used as it exhibited maximum ionic conductivity. The $LiCr_{0.01}Mn_{1.99}O_4$ spinel compound was prepared from the stoichiometric mixture of $LiOH \cdot H_2O$, $(NH_4)_2Cr_2O_7$ and $(CH_3CO_2)_2Mn \cdot 4H_2O$. The finely ground mixture was burned at 250 ° C for 20 h and then calcined at 800 °C for 24 h with intermediate grinding.

The composite cathode was prepared by brush-coating a slurry of 85% of $LiCr_{0.01}Mn_{1.99}O_4$, 5% of poly(vinyledene difluoride-hexafluoropropylene) and 10% acetylene black in 1-methyl-2-pyrrolidinone on an aluminum substrate and drying in a vacuum oven at 120 °C for 12 h. Lithium foil was used as the anode. $LiCr_{0.01}Mn_{1.99}O_4$/CPE/Li cells were assembled using the procedure as reported elsewhere [14–16]. The structural properties of the nanocrystalline Cr^+-doped $LiMn_2O_4$ and its cycling behavior with non-aqueous electrolyte (1 M $LiPF_6$ in EC: DMC 2:1 by vol.) have already been reported [15].

Table 1. The composition of the polymer, lithium salt, filler content and transport number of the membranes prepared with different sizes of the fillers

Sample	Polymer wt.%	Li-salt wt.%	Fille rwt.%	Transport number (t_{Li}^+)			
				$LiClO_4$		LiBETI	
S1	95	5	0	0.30	0.35	0.38	0.38
S2	92.5	5	2.5	0.40	0.45	0.47	0.48
S3	90	5	5.0	0.45	0.47	0.48	0.49
S4	87.5	5	7.5	0.50	0.54	0.57	0.58
S5	85	5	10.0	0.56	0.60	0.65	0.70
S6	82.5	5	12.5	0.52	0.59	0.63	0.64
S7	80	5	15.0	0.52	0.58	0.63	0.63

3. Results and discussions

3.1. *XRD-analysis*

The XRD patterns of PVdF–HFP polymer and PVdF–HFP + AlO $[OH]_n$ (of nano sized) + $LiN(C_2F_5SO_2)_2$ composite polymer electrolyte membranes are displayed in Figure 1(a, b) respectively. The same peak profile was also observed for films with filler of micron size (not shown in the figure). No discernible changes could be observed in the peak pattern when the filler size was changed from 40 nm to 7 μm. The crystalline peaks of PVdF are observed at 2θ = 18.2, 20, 26.6 and 38, which correspond to (1 0 0) (0 2 0), (1 1 0) and (0 2 1). This confirms the partial crystallization of PVdF units in the copolymer and gives a semi- crystalline structure of PVdF–HFP [28]. The crystallinity of the polymer is considerably decreased upon the addition of the inert

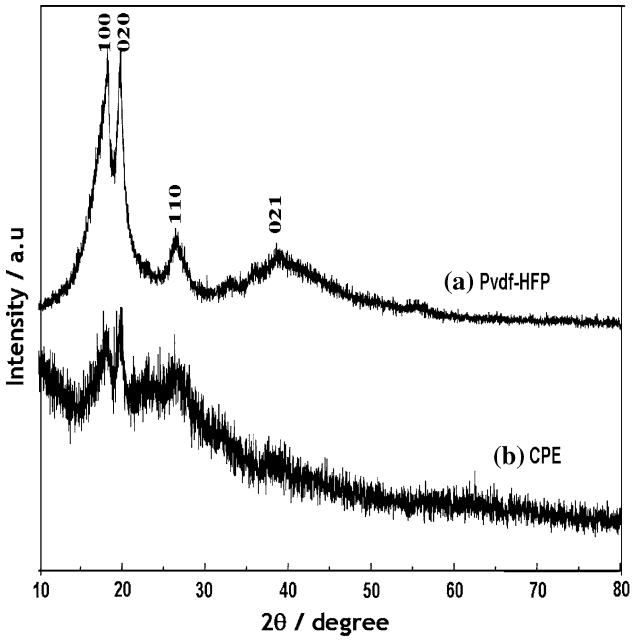

Fig. 1. XRD patterns of (a) PVdF–HFP (b) PVdF–HFP + 10% $AlO[OH]_n$ (nanosized) + $LiN(C_2F_5SO_2)_2$.

filler and lithium salt. It is clear from Figure 1(b) that the intensity of the crystalline peaks decreases and broadens. This reduction in crystallinity upon the addition of inert filler is attributed to small particles of inert filler which change the chain re-organization and offers higher ionic conduction [28]. These results agree with those for PAN-$LiClO_4$-α-Al_2O_3 [23] and the TiO_2 incorporated PMMA/PEGDA blend composite electrolyte system [24].

3.2. *Ionic conductivity*

Figure 2 (a, b) display the temperature dependence of composite polymer electrolyte membranes comprising PVdF–HFP + $AlO[OH]_n$ (nm sized) + $LiN(C_2F_5SO_2)_2$ and PVdF–HFP + $AlO[OH]_n$ (micron sized) + $LiN(C_2F_5SO_2)_2$ as a function of filler content respectively. The ionic conductivity of the composite polymer electrolyte increases with increase in temperature and also increases with increase in filler content. The ionic conductivity of the polymer membrane is increased by one order of magnitude upon the addition of filler in the polymer host (Sample S2). The ionic conductivity also increases with increase in filler content up to 10 wt.% (sample S1–S5) and then decreases with increase in filler content. A similar trend was observed for the $LiClO_4$ added systems as displayed in Figure 3 (a, b). These results agree with those reported earlier in which γ-Al_2O_3 was used as filler in PEO-based electrolytes [29]. As commonly found in composite materials the conductivity is not a linear function of filler concentration. Hence, an apparent enhancement in conductivity is seen in both cases. On the other hand, when the concentration of the filler is increased the dilution effect predominates and the conductivity decreases (sample S6) [21].

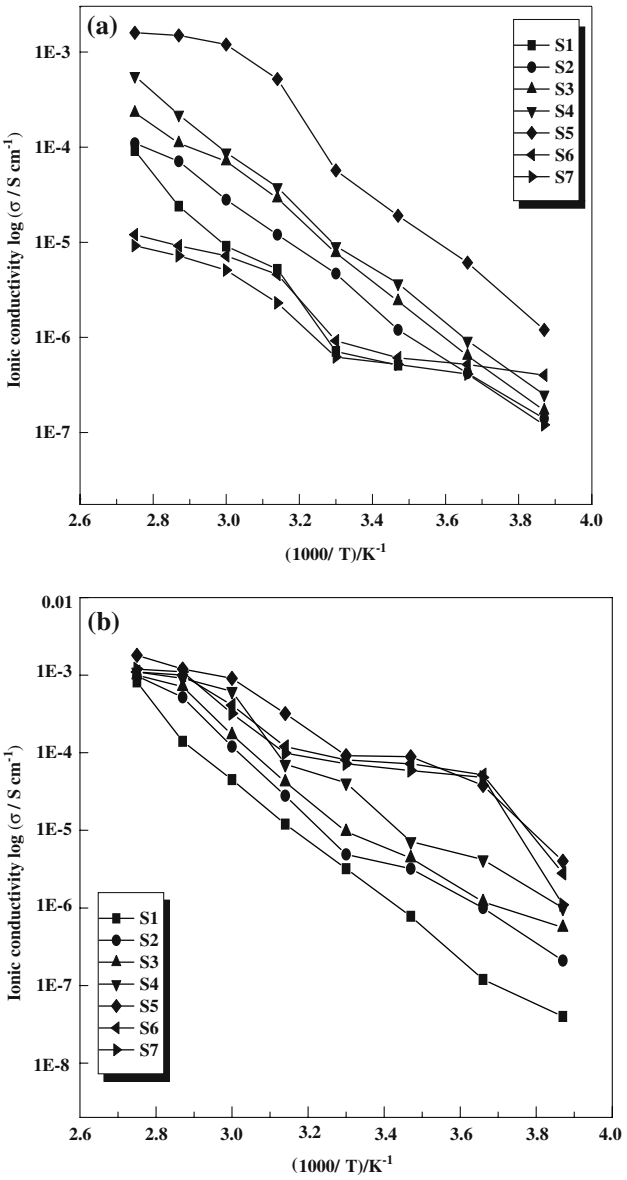

Fig. 2. (a) Temperature dependence of PVdF–HFP + $AlO[OH]_n$ (nano sized) + $LiN(C_2F_5SO_2)_2$ as a function of filler content. (b) Temperature dependence of PVdF–HFP + $AlO[OH]_n$ (micron sized) + $LiN(C_2F_5SO_2)_2$ as a function of filler content.

Thus the maximum conductivity is achieved in the concentration region 8–10 wt%. According to Appetecchi and co-workers [21] NMR studies show that the local dynamics of the lithium ions, in particular lithium mobility, is not changed by the filler which supports the idea that the enhancement of conductivity by adding a filler is caused by stabilizing and increasing the fraction of amorphous phase. Our XRD result also substantiates this. However, this aspect does not hold good solely for the enhancement of conductivity where the polymer is amorphous by nature. According to Croce et al. [30], the Lewis acid groups of the added inert filler may compete with the Lewis-acid lithium cations for the formation of complexes with the PEO chains as well as the anions of the added lithium salt. Subsequently, this results in structural modifications on the filler surfaces

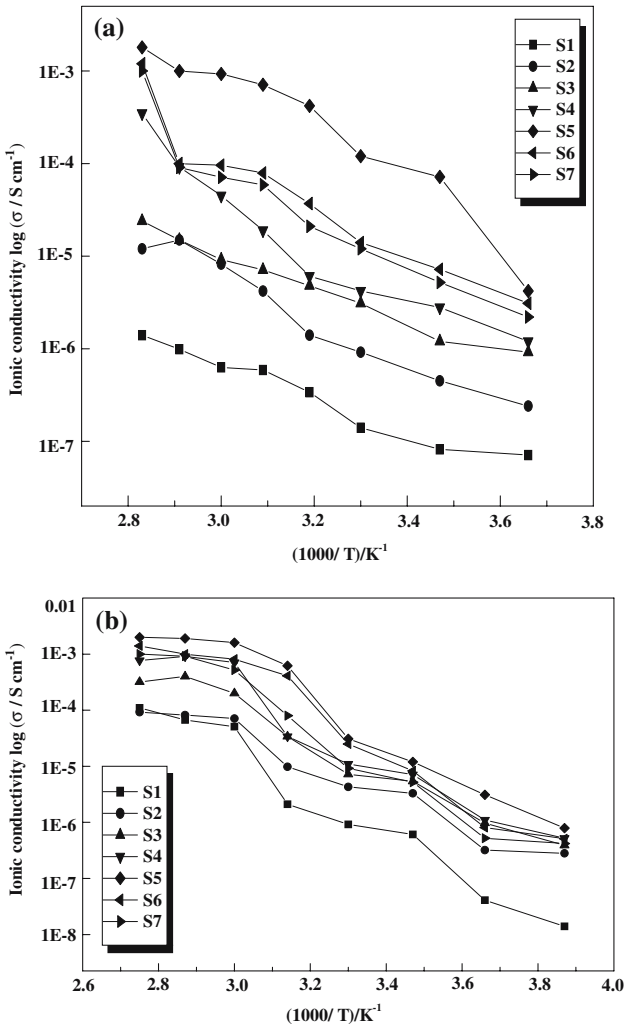

Fig. 3. (a). Temperature dependence of PVdF–HFP + $AlO[OH]_n$ (40 nm) + $LiClO_4$ as a function of filler content. (b). Temperature dependence of PVdF–HFP + $AlO[OH]_n$ (7 microns) + $LiClO_4$ as a function of filler content.

due to the specific actions of the polar surface groups of the inorganic filler. The interaction between Lewis acid–base centers and electrolytic species lowering the ionic coupling and promotes salt dissociation via a sort of ''ion- filler complex'' formation. In the present study the filler, $AlO[OH]_n$, which has a basic center can react with the Lewis acid centers of the polymer chain and these interactions lead to the reduction in crystallinity of the polymer host. This effect explains the observed enhancement in ionic conductivity for both systems [31].

3.2.1. *Effect of anion*

While comparing the ionic conductivity data of the composite polymer electrolytes from Figures 2(a) with 3(a) and 2(b) with 3(b) the ionic conductivity of the CPE which possesses $LiN(C_2F_5SO_2)_2$ as salt exhibits higher conductivity than the CPE containing $LiClO_4$. At high temperatures, the conductivity of $LiN(C_2F_5SO_2)_2$ and $LiClO_4$ are more or less same. At lower temperature, the salt $LiN(C_2F_5SO_2)_2$ having a lower T_g value (T_g = 206 °C) had higher conductivity than the salt $LiClO_4$ with a higher value of T_g. (T_g = 211 °C) [31–33]. Lattice energies and salt association constants are only rough guides to predict conductivity order in polymer electrolytes. Although conductivities of the solid polymer electrolytes were observed to increase at low salt concentrations the relative order changed at higher salt concentrations [34, 35]. Similarly, association constants are concentration dependent in a manner that depends on the salt [35]. In low dielectric solvents, the constants of formation of ion pairs at infinite dilution did not correlate with conductivity trends of the anions [36]. However, there is often an approximate correlation between salt association at both low and high salt concentrations.

The conductivity order based on the anion type is not fully understood for both liquid and polymer electrolytes for lithium batteries. The conductivity can be affected by the ionic mobility, ion–ion interactions, anion size, lattice energies and salt dissociation and also anion polarization, all of which depend on salt concentration. However, in the present study the order of conductivity based on the type salt is consistent with other reports for PEO [30] and PEGDME/PVdF–HFP blend electrolytes [31].

3.3. *Transference number*

The lithium transference number, t_{Li}^+, measurement has been used as complimentary tool to impedance analysis. The transference number, t_{Li}^+, for the composite polymer electrolytes are displayed in Table 1. This table depicts the results in terms of numerical values of t_{Li}^+. According to Bruce et al. [35] the transference numbers may equally be affected by the interfacial properties with lithium metal anodes. An apparent increase in the transference number, t_{Li}^+ (Table 1) is observed when passing from the filler-free to the filler incorporated composite electrolytes. More interestingly, the transference number of the nanofiller incorporated composite polymer electrolytes exhibit higher values than the electrolytes of micron size which, further supports the ionic conductivity results.

3.4. *Compatibility*

It is generally known that the reactivity of lithium electrode affects lithium metal anode/electrolyte interface due to uncontrolled passivation phenomena which leads to the formation of a thick and non-uniform surface layers [36]. These layers cause an uneven lithium deposition during the charging process which in turn eventually leads to dendritic growth and cell short-circuiting. Therefore the interfacial properties of lithium metal anodes with composite polymer electrolytes also play a vital role in practical applications. In the present study the influence of the particle size of the inert filler and the type of lithium salt on the Li/CPE/Li cells have been analyzed at 70 °C. The sample S5 was used for this study as it exhibited highest ionic conductivity among

the samples studied. The variation of the interfacial resistance, "R_i" as a function of time for the Li/CPE with $LiN(C_2F_5SO_2)_2$ as salt/Li symmetric cells is displayed in Figure 4. It is clear from Figure 4 that the interfacial resistance values are considerably reduced upon the addition of inter filler (i.e., the interfacial values are lower than the filler-free electrolytes). A similar trend was observed for the composite polymer electrolyte containing $LiClO_4$ as salt (Figure 5). The addition of the filler traps any remaining traces of organic solvent impurities and this may account for the enhanced interfacial stability of the composite polymer electrolytes and the passivation process may basically involve a reaction between the lithium metal and the anions of the lithium salt with the formation of a thin, compact inorganic layer which favors good lithium cyclability [37]. It is observed, from Figures 4 and 5 that the polymer electrolyte containing $LiClO_4$ as salt is more suitable when lithium metal is used as anode. However, on the other hand the film with $LiN(C_2F_5SO_2)_2$ as salt exhibits higher interfacial resistance. The poor compatibility of polymer electrolytes containing fluorinated lithium salts with the lithium metal anode may be attributed to the following reasons. As confirmed by XPS analysis the amount of the fluorine substances on the lithium surface increases accordingly to the storage time [38, 39]. An important reason for the increase in "R_i" is likely to be the formation of fluorine compounds on the lithium surface [38, 39]. Also of importance is that the composite polymer electrolyte with nanosized fillers exhibits better compatibility than the filler of micron size. According to Kumar et al. [40] nano sized inert fillers are more compatible than fillers of micron size. As depicted in Figure 6, the inert particles, depending on the volume fraction, tend to minimize the area of lithium electrode exposed to polymers containing O, OH-species and thus reduce the passivation process. It is also likely that smaller size particles for a similar volume fraction of the ceramic phase impart improved performance as compared to larger size particles because they cover more surface area [40]. The formation of an insulated layer of ceramic particles at the electrode surface is probable at higher volume fraction of the passive ceramic phase. This insulating layer will impede electrode reactions. This may very well have happened when an excessive amount of the passive ceramic phase were introduced into the polymer matrix. Also the PVdF–HFP co-polymer reacts with lithium at ambient and elevated temperatures. The growth of interfacial resistance does not follow a regular trend for all the samples studied. After, 120 h the resistance values

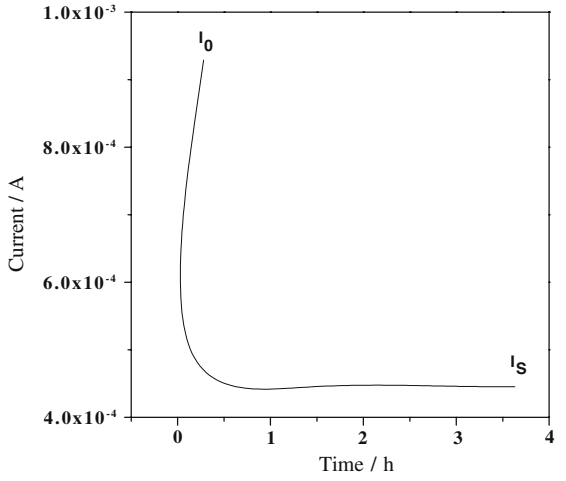

Fig. 4. Current relaxation plot for transference number measurement of CPE.

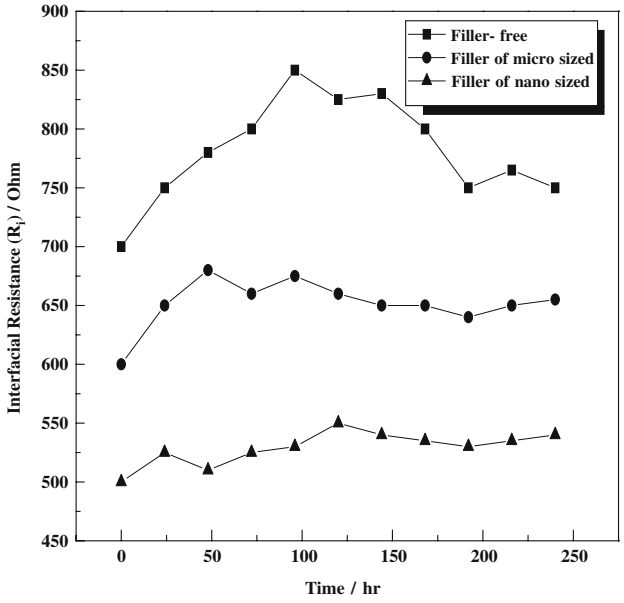

Fig. 5. Interfacial resistance 'R_i' as a function of time for the symmetric cells Li/CPE/Li. Salt: $LiN(C_2F_5SO_2)_2$.

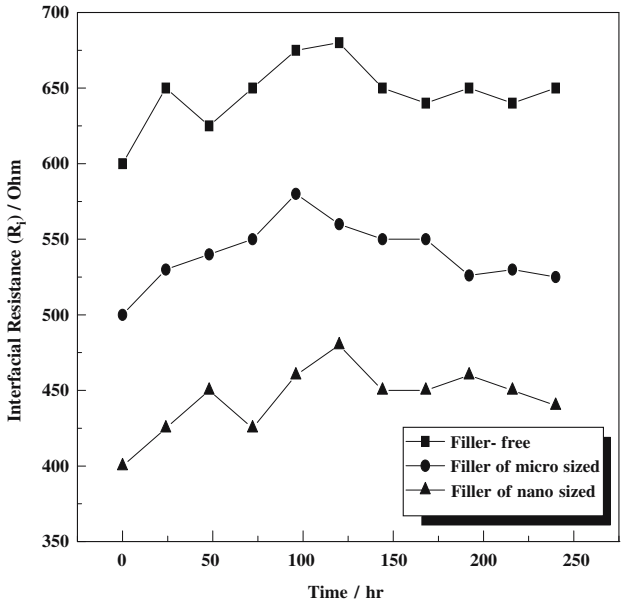

Fig. 6. Interfacial resistance 'R_i' as a function of time for the symmetric cells Li/CPE/Li. Salt: $LiClO_4$.

remain unchanged. This may be due to the fact that the morphology of the passive film changes with time to finally acquire a non-compact, possibly porous, structure [27].

3.5. *Charge-Discharge studies*

The cycling behavior of $LiCr_{0.01}Mn_{1.99}O_4$/CPE/Li cells at 70 °C is shown in Figure 7. According to Sun et al., [41] the spinel $LiMn_2O_4$ is more compatible with polymer electrolytes than layered $LiCoO_2$ and is favored as cathode material due to lower price and the lesser toxicity of manganese. However, the discharge capacity of $LiMn_2O_4$ cells decreases rapidly upon repeated cycling due to Jahn-/Teller distortion in the manganese oxide spinel structure. This leads to a larger capacity fade upon prolonged cycling. It has been suggested that the fade in capacity in the 3 V region is due to this distortion and that the reduction in capacity in the 4 V region is due to both dissolution of spinel into the electrolyte and decomposition of the electrolyte [42, 43]. It has been shown that the substitution of a small amount of a dopant ion in place of Mn ions can improve the cyclability of $LiMn_2O_4$. It is reported in our earlier study that, $LiCr_{0.01}Mn_{1.99}O_4$ exhibited excellent capacity retention when non-aqueous electrolyte was used. Hence in the present study, composite electrolyte sample S5 was employed as it has been found to be optimal from the ionic conductivity and compatibility points of view. The lower and upper cut- off voltages of the cell were fixed as 2.8 V and 4.2 V respectively for the fear of decomposition of the electrolyte. The cells were cycled at 0.2C rate. The polymer cell composed of $LiCr_{0.01}Mn_{1.99}O_4$/PVdF–HFP–AlO[OH]$_n$ 10% (nm sized)-$LiN(C_2F_5SO_2)_2$/Li and $LiCr_{0.01}Mn_{1.99}O_4$/PVdF–HFP–AlO[OH]$_n$ 10% (micron sized)-$LiN(C_2F_5SO_2)_2$/Li delivered initial and final discharge capacities of 125, 121, 120 and 115 mAh g^{-1} after 25 cycles and their fade in capacity per cycle of the cells was 0.2 and 0.24 mAh g^{-1}, respectively. Similarly those comprising $LiCr_{0.01}Mn_{1.99}O_4$ /PVdF–HFP–AlO[OH]$_n$ 10% (nm sized)–$LiClO_4$/Li and $LiCr_{0.01}Mn_{1.99}O_4$/PVdF–HFP–AlO[OH]$_n$ 10% (micron sized)–$LiClO_4$/Li delivered initial and final discharge capacities of 130, 128, 126 and 123 mAh g^{-1} after 25 cycles and their fade in capacity per cycle was 0.16 and 0.2 mAh g^{-1}, respectively. The cell with the membrane of micron sized filler undergoes slightly higher fade in capacity after 15 cycles and this is attributed to the high interfacial resistance of the system, Li/PVdF–HFP–AlO[OH]$_n$ 10% $LiN(C_2F_5SO_2)_2$/Li as depicted in Figure 8. A similar observation was reported by Yamamoto et al. [18] for PEO-$LiBF_4$–$BaTiO_3$ systems. Generally, the fade in capacity for $LiMn_2O_4$ – based systems is attributed to Jahn-Teller distortion, lattice instability, manganese dissolution, oxidation of electrolyte, formation of oxygen rich spinel, lattice site exchange between lithium and manganese ions and particle disruption [42–44].

In the present case, the manganese is partially substituted by the Cr^- ion which led to higher capacity retention when non-aqueous electrolyte was used [15]. Hence in the present case the fade in capacity is attributed mainly to the higher interfacial resistance of the composite polymer electrolyte with lithium metal anode as depicted in Figures 8 and 4. As evidenced by Song et al. [3] and Ismail et al. [45] fluorinated polymers are not chemically stable towards lithium owing to the interfacial reaction between lithium and fluorine that results in the formation of LiF and subsequently leads to poor cycling performance [46, 47].

4. Conclusions

PVdF–HFP composite polymer electrolytes with AlO[OH]$_n$ inert filler and $LiN(C_2F_5SO_2)_2$/$LiClO_4$ as lithium salt were prepared. The crystallinity of the

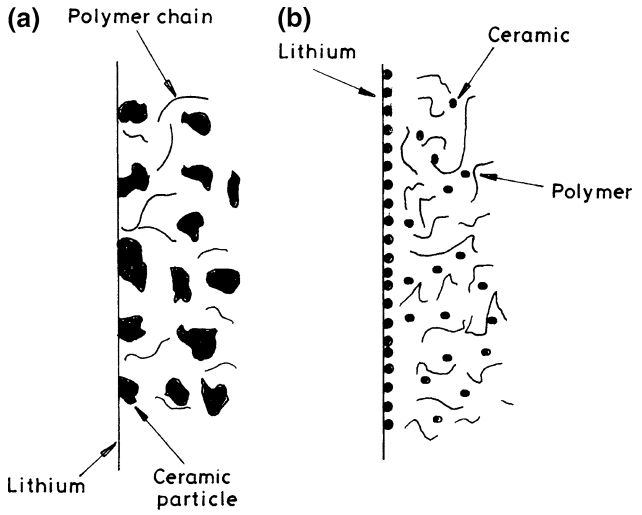

Fig. 7. A schematic representation of polymer chain and inert filler in a CPE Filler of (a) micron size (b) nano size. (Ref. 39).

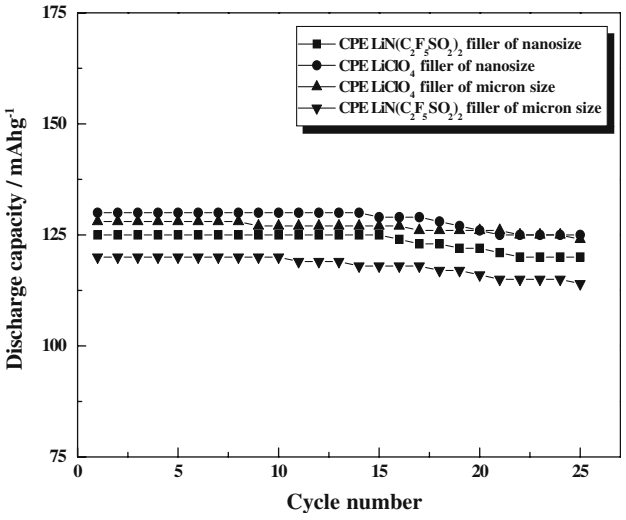

Fig. 8. Cycling behavior of $LiCr_{0.01}Mn_{1.99}O_4$/CPE/Li cells at 70 °C.

polymer host was considerably reduced upon addition of filler and this filler acts as a 'solid plasticizer' to enhance the conduction mechanism and also provides better interfacial properties towards the lithium metal anode. The cycling behavior of $LiCr_{0.01}Mn_{1.99}O_4$/CPE/Li cells shows convincing results at elevated temperature and may be employed as a separator for lithium polymer batteries for hybrid electric vehicle operations.

Acknowledgements

One of the authors (A.M.S) thanks the Korean Federation of Science and Technology Societies (KOFSTS) for offering a visiting scientist fellowship under the Brain pool program.

References

1. B. Scrosati, *Applications of Electroactive Polymers* (Chapman and Hall, London, 1993).
2. P.G. Bruce, *Electrochim. Acta*. **40** (1995) 2077.
3. J.Y. Song, Y.Y. Wang and C.C. Wan, *J. Electrochem. Soc*. **77** (2000) 183.
4. G.B. Appetecchi, S. Scaccia and S. Passerini, *J. Electrochem. Soc*. **147** (2000) 4448.
5. A. Manuel Stephan, *Eur. Polym. J*. **42** (2006) 21.
6. H.J. Rhoo, H.T. Kim, J.K. Park and T.S. Huang, *Electrochim. Acta* **42** (1997) 1571.
7. A. Manuel Stephan, T.P. Kumar, R.T. Karan, N.G. Renganathan, S. Pitchumani, J. Shrisudersan and N. Muniyandi, *Solid State Ionics* **130** (2000) 123.
8. A. Manuel Stephan, S. Gopukumar, N.G. Renganathan and M. Anbu Kulandainathan, *Eur. Polym. J*. **41** (2005) 15.
9. A. Manuel Stephan, T.P. Kumar, R.T. Karan, N.G. Renganathan, S. Pitchumani and N. Muniyandi, *J. Power Sources* **89** (2000) 80.
10. J.-M. Tarascon, A.S. Gozdz, C. Schmutz, F. Shokoohi and P.C. Warren, *Solid State Ionics* **86–88** (1996) 49.
11. A. Manuel Stephan, H. Kataoka and Y. Saito, *Macromolecules* **34** (2001) 6955.
12. A. Manuel Stephan and Y. Saito, *Solid State Ionics* **148** (2002) 475.
13. Y. Saito, A. Manuel Stephan and H. Kataoka, *Solid State Ionics* **160** (2002) 149.
14. A. Manuel Stephan and D. Teeters, *J. Power Sources* **119–121** (2003) 460.
15. A. Manuel Stephan and D. Teeters, *Electrochim. Acta*. **48** (2003) 2143.
16. A. Manuel Stephan, S. Gopu Kumar, N.G. Renganathan D. Teeters, *Mater. Chem. & Phys*. **85** (2004) 6.
17. J.Y. Song, Y.Y. Wang and C.C. Wan, *J. Electrochem. Soc*. **147** (2000) 3219.
18. Q. Li, N. Imanishi, A. Hirano, Y. Takeda and O. Yamamoto, *J. Power Sources* **110** (2002) 38.
19. Q. Li, T. Itoh, N. Imanishi, A. Hirano, Y. Takeda and O. Yamamoto, *Solid State Ionics* **159** (2003) 97.
20. G.B. Appetecchi, J. Hassoun, J.B. Scrosati, F. Croce, F. Cassel and M. Salomon, *J. Power Sources* **124** (2003) 246.
21. G.B. Appetecchi, F. Croce, L. Persi, F. Ronci, B. Scrosati F. Soavi, A. Zanelli, F. Alessadrini and P.P. Prosini, *J. Electrochem. Soc*. **145** (1998) 4126.
22. B. Kumar, L. Scanlon, R. Marsh, R. Mason, R. Higgins R. Baldwin, *Electrochim. Acta* **46** (2001) 1515.
23. Z. Wang, H. Huang and L. Chen, *Electrochem. Solid State Lett*. **6** (2003) E40.
24. H.S. Kim, K.S. Kum, W.I.I. Cho, B. Woncho and W.H. Rhee, *J. Power Sources* **124** (2003) 221.
25. V.D. Noto and V. Zago, *J. Electrochem. Soc*. **151** (2004) A216.
26. W. Krawiec, L.G. Scanlon, J.P. Fellner, R.A. Vaia, S. Vasudevan and E.P. Giannelis, *J. Power Source* **54** (1995) 310.
27. G.B. Appetecchi, F. Croce and B. Scrosati, *Electrochim. Acta* **40** (1995) 991.
28. D. Saika and A. Kumar, *Electrochim. Acta* **49** (2004) 2581.
29. X. Qian, N. Gu, Z. Cheng, X. Yang, E. Wang and S. Dong, *Electrochim. Acta* **46** (2001) 1829.
30. F. Croce, L. Perci, B. Scrosati, F. Serraino-Fiory, E. Plichta and M.A. Hendrickson, *Electrochim. Acta* **46** (2001) 2457.
31. W. Wieczorek, J.R. Steven and Z. Florjanczyk, *Solid State Ionics* **85** (1996) 67.
32. I.W. Cheung, K.B. Chin, E.R. Greene, M.C. Smart, S. Abbrent, S.G. Greenbaum, G.K.S. Prakash and S. Surampudi, *Electrochim. Acta* **48** (2003) 2149.
33. K.M. Abraham, Z. Jiang and B. Carroll, *Chem. Mater*. **9** (1997) 1978.
34. N. Kobayashi, M. Uchiyama, K. Shigehara and E. Tsuchida, *J. Phys. Chem*. **89** (1985) 987.
35. S. Besner, A. Valee, G. Bouchard and J. Prud'homme, *Macromolecules* **25** (1992) 6480.
36. N. Kobayashi, S. Sunaga and R. Hirohashi, *Polymer*. **33** (1992) 3044.
37. Y. Aihara, T. Bando, H. Nakagawa, H. Yoshida, K. Hayamizu E. Akiba and W.S. Price, *J. Electrochem. Soc*. **151** (2004) A119.
38. J. Evans, C.A. Vincent and P.G. Bruce, *Polymer*. **28** (1987) 2324.
39. F. Croce and B. Scrosati, *J. Power Sources* **43** (1993) 9.
40. F. Croce, L. Perci, B. Scrosati, F. Serraino-Fiory, E. Plichta and M.A. Hendrickson, *Electrochim. Acta* **46** (2001) 2457.
41. Y.K. Sun and S.H. Jin, *J. Mater. Chem*. **8** (1998) 2399.
42. D.H. Jiang, J.Y. Shin and S.M. Oh, *J. Electrochem. Soc*. **143** (1996) 2204.
43. Y. Xia, Y. Zhou and M. Yoshio, *J. Electrochem. Soc*. **144** (1997) 2593.
44. G.T.K. Fey, C.Z. Lu and T. Prem Kumar, *J. Power Sources* **115** (2003) 332.
45. I. Ismail, A. Noda, A. Nishimoto and M. Watanabe, *Electrochim. Acta* **46** (2001) 1595.
46. K. Kanamura, H. Tamura, S. Shiraishi and Z. Takehara, *J. Electrochem. Soc*. **142** (1995) 340.
47. B. Kumar and L.G. Scanlon, *J. Power Sources* **52** (1994) 261.